Observation of shock waves in a large Bose-Einstein condensate

R. Meppelink, S. B. Koller, J. M. Vogels, and P. van der Straten

Atom Optics and Ultrafast Dynamics, Utrecht University, 3508 TA Utrecht, The Netherlands

E. D. van Ooijen,[*] N. R. Heckenberg, and H. Rubinsztein-Dunlop

School of Mathematics and Physics, The University of Queensland, Queensland 4072, Australia

S. A. Haine and M. J. Davis

School of Mathematics and Physics, ARC Centre of Excellence for Quantum-Atom Optics, The University of Queensland, Queensland 4072, Australia

We observe the formation of shock waves in a Bose-Einstein condensate containing a large number of sodium atoms. The shock wave is initiated with a repulsive blue-detuned light barrier, intersecting the Bose-Einstein condensate, after which two shock fronts appear. We observe breaking of these waves when the size of these waves approaches the healing length of the condensate. At this time, the wave front splits into two parts and clear fringes appear. The experiment is modeled using an effective one-dimensional Gross-Pitaevskii-like equation and gives excellent quantitative agreement with the experiment, even though matter waves with wavelengths two orders of magnitude smaller than the healing length are present. In these experiments, no significant heating or particle loss is observed.

I. INTRODUCTION

The realization of Bose-Einstein condensates (BECs) in dilute atomic gases [1] provides the opportunity for the study of nonlinear matter wave dynamics. Many experiments on both the statics and dynamics of BECs have shown that experiments can often be modeled accurately by solving the mean-field Gross-Pitaevskii equation (GPE) [2–13]. For example, it has successfully been used to model experiments on interferometry [2,13], soliton formation [4,7], four wave mixing [5], atom laser outcoupling [9–11], sound propagation, and superfluidity [2] to name a few. However, the Gross-Pitaevskii equation is not an exact description of a Bose-Einstein condensate, but instead it is expected to be a good approximation for condensates that contain a relatively large number of particles and are not undergoing violent dynamics [14,15]. Thus, it is of interest to experimentally probe the limits of validity of the GPE in describing the dynamics of Bose-Einstein condensates.

The well-known "Bosenova" (explosive collapse of a BEC) experiment of Donley *et al.* [16] is one situation where the validity of the GPE might be questioned, combining a small number of atoms with violent dynamics. The experiment began with a near ideal ^{85}Rb condensate of a few thousand atoms in its ground state before the atomic scattering length was manipulated using a Feshbach resonance to being attractive. The BEC was observed to collapse, emitting high-energy jets and bursts of atoms. A number of computational studies have shown good qualitative agreement with the experimental observations [17–19]. However, careful quantitative studies have indicated that at the most basic level, there is quantitative disagreement with the experimental data. Savage *et al.* showed that the experimentally measured collapse time is typically 25% *shorter* than predicted by simulations of the GPE [20]. Going beyond mean-field theory and including the first-order quantum corrections to the dynamics was shown to make little difference to the numerical results [21,22]. A second group of experiments by the same group found evidence for the formation of repulsive bright solitary waves in the condensate collapse [23]. However, modeling this experiment with the GPE is unable to reproduce this experimental finding [24].

Another example where the GPE has successfully modeled results of violent experiments is in the formation of quasi-one-dimensional (1D) bright solitons as reported in Refs. [25,26]. Both of these experiments involve a sudden change to an attractive scattering length. It has been shown [7] that the GPE can be used to successfully model these experiments. However, in this case, the three-body recombination, which is not included in the GPE derivation, plays a nontrivial role in the dynamics, and the GPE must be modified by the addition of phenomenological damping terms in order to agree with these experiments.

Another situation exhibiting violent dynamics in the solution of the GPE without dissipation is in the generation of shock waves. Damski [27] calculated the 1D GPE dynamics, following the introduction and sudden removal of an attractive dimple potential in the center of a harmonically trapped elongated BEC. The localized density bulge splits into two pulses, which propagate toward the ends of the condensate. Due to the density-dependent speed of sound in the system, the center of the pulse catches up to the front, creating a shock, and at this point the calculations develop a strong fringe pattern with a spacing on the order of the healing length corresponding to classical wave breaking. However, Damski speculated that in a physical system, the Gross-Pitaevskii equation would become invalid at this point and this would not be observed in an experiment [28,29].

_____
[*]ooijen@physics.uq.edu.au

A similar situation occurs when there is a rapid change in the magnitude of the scattering length. Perez-Garcia *et al.* performed a theoretical analysis of this situation and found similar wave breaking phenomena [30]. Theoretical analysis of the motion of an obstacle through a Bose-Einstein condensate has shown that shock waves form when the obstacle exceeds the sound speed of the fluid [31–34].

Recently, a number of experiments have been performed that have observed phenomena related to wave breaking in a Bose-Einstein condensate. The first experiments were by Dutton *et al.* [6]. They used the slow light mechanism to create a defect in the condensate, which was much narrower than the healing length. This defect created dark solitons, which shed high frequencies traveling at different velocities. The wave front of the propagating solitons eventually became curled and decayed into vortex pairs.

Simula *et al.* [35] blasted a hole in a rapidly rotating oblate BEC using a repulsive dipole potential and found qualitative agreement between their experimental observations and numerical calculations of the GPE. This was followed by Hoefer *et al.*, who performed similar experiments on a stationary and slowly rotating oblate BEC, and made the connection to dispersive shock waves in the GPE [36]. They found that this wave breaking phenomenon can be described by the Gross-Pitaevskii equation [37]. However, to obtain quantitative agreement between the simulations and the experimental observations, they found that they had to use the laser width as a fitting parameter. In one situation, agreement was obtained with a value of 1.5 times larger than in the experiment, but in another it was required to be half as large, suggesting that this is not a systematic error but something more fundamental.

The purpose of this paper is to generate shock waves in a large number elongated BEC and to perform a quantitative comparison with simulations of an effective 1D GPE as a test of its validity in extreme conditions. We observe no indication of heating or particle loss and conclude that, even at these relatively high-energy scales, the GPE is valid for the time of the experiment. Soon after the experimental data for this work was taken, related work was reported by Chang *et al.* [38]. They also found good agreement with the GPE. However, these experiments were performed at significantly lower-energy scales, where agreement with the GPE is expected, and, hence, they did not perform a detailed investigation of the fringe spacing and possibility of heating [39].

II. EXPERIMENT

In our experiment, we begin with an almost pure sodium BEC containing up to 100 million atoms in the $|F, m_F\rangle = |1, -1\rangle$ hyperfine state. The atoms are magnetically confined in a clover leaf trap with harmonic trapping frequencies of 97 Hz in the radial direction and 3.9 Hz in the longitudinal direction [40]. For the condensate, this corresponds to a chemical potential of 214 nK and Thomas-Fermi widths of 20 μm and 506 μm in the radial and axial directions, respectively. To create the initial disturbance, we turn on a repulsive blue-detuned laser beam focused in the middle of the BEC, intersecting the cloud in the longitudinal direction. The focus has
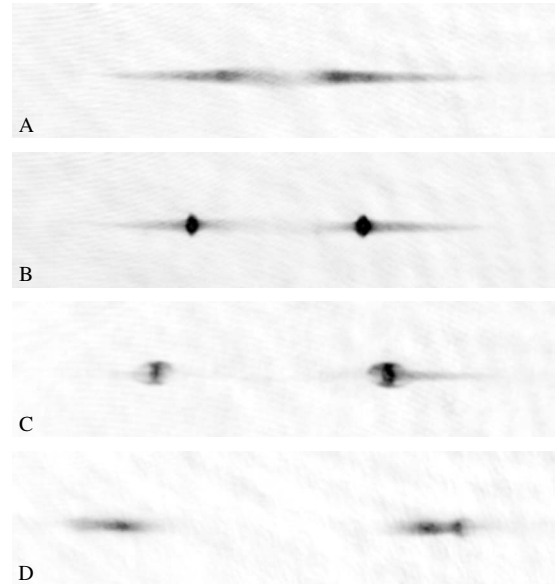

FIG. 1. Phase contrast images of the BEC in the trap for (A)–(D) $t = 2$, 5, 8, and 15 ms after turning on the blue-detuned laser beam. The image size is 1200×300 μm.

a waist of 90 ± 11 μm($1/e^2$) and a wavelength λ_L, tunable from 567 to 584 nm, where the power can be switched within 10 μs. At $t = 0$, the blue-detuned laser is turned on suddenly with the magnetic trap still on and after variable times the cloud is imaged in the trap. Note that the waist of the laser focus is much smaller than the axial width of the condensate and much larger than the radial widths, suggesting that most of the dynamics will occur along the axial dimension.

A. Case 1

For the first set of experiments, we make use of phase-contrast in-trap imaging [41]. The detuning of the imaging laser is chosen such that a 2π phase shift is accumulated for the largest atom cloud density. The resolution is 3×3 μm^2 and the images are recorded with a charge-coupled device (CCD) camera (Apogee AP1E). Figure 1 shows the in-trap CCD images for a BEC with 50 million atoms, corresponding to a chemical potential $\mu = 162$ nK imaged after $t = 2$, 6, 8, and 15 ms, respectively. The power for the repulsive laser beam used is 78 mW with a wavelength of 579 nm, resulting in a repulsive barrier of 12.6 μK. For all experiments, the scattering of photons from the laser can be neglected. The first image shows the splitting of the cloud induced by the switch on of the repulsive barrier. The density profile of the BEC results in a gradient in the speed of sound of the condensate v_c as $v_c \sim \sqrt{n}$. As a consequence, as the wave fronts induced by the lasers travel from the center toward the edge of the condensate width, the back of the pulse catches up to the front, resulting in steepening of the wave (self-steepening). This is clearly observed in the second image. The last two images show that the wave breaks into two parts after the maximum density gradient has been reached.

B. Case 2

As the size of the fringes in the data set above was much smaller than the resolution of the imaging system, the experi-
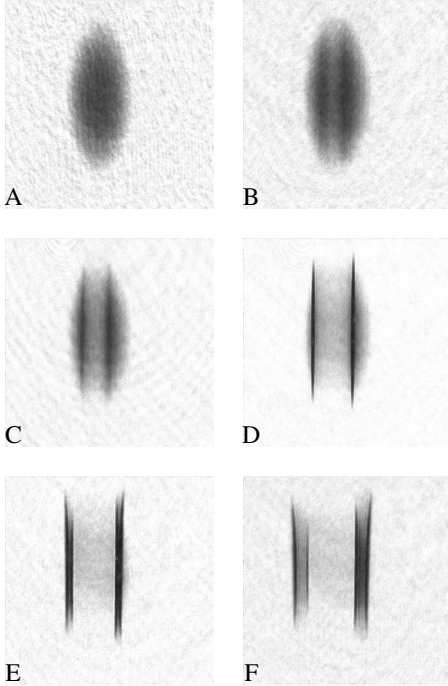
FIG. 2. Absorption images of a 70 ms expanded BEC for (A)–(F) $t=0$, 1, 2, 6, 13, and 25 ms after turning on the repulsive barrier. The size of the images is 2304×1536 μm.

ment was repeated and imaged using a 70 ms time-of-flight expansion to enlarge the detailed features of the condensate. This free expansion time was chosen in such a way that the full CCD array is used to obtain the maximum resolution. Figure 2 shows the images for a smaller condensate of 18 million atoms for an evolution time in the trap of 0, 1, 2, 6, 13, and 25 ms, respectively. In this situation, we use a repulsive laser beam with a power of 21 mW and a wavelength of 569 nm, corresponding to a repulsive potential barrier with a height of 0.43 μK.

The images in Fig. 2 indicated that it takes longer for the buildup of the wave front for a smaller BEC and a weaker repulsive barrier. It can be seen that the shock front splits into two parts, where pronounced fringe patterns appear. Fourier analysis on the last image shows a fringe size of 6 ± 1 μm. Integration over the entire pixel array shows a 2.7% fluctuation in the number of atoms over a evolution time of 30 ms, suggesting that losses due to any potential heating are negligible. Frames (E) and (F) show that there is a slight curvature of the wave fronts, suggesting that the outer edge of the wave front has traveled faster than the center.

III. NUMERICAL SIMULATIONS

We now turn to numerical modeling these experiments. Ideally, we would do so with a fully three-dimensional simulation of the Gross-Pitaevskii equation. However, even making use of the cylindrical symmetry we find that the simulation parameters for such a large BEC are too demanding for numerical simulation with the computational resources we have available. To proceed, we have made use of the fact that

the system has cylindrical symmetry and a high aspect ratio and reduced the problem to simulating the one-dimensional nonpolynomial Gross-Pitaevskii equation (NPGPE) as derived by Salasnich *et al.* [42]. This assumes a variational Gaussian profile for the wave function in the radial direction, whose width $\sigma(z)$ is dependent on the local one-dimensional density. This is to allow for the "bulging" in the radial direction due to the mean-field interaction to be included. The result is a 1D Gross-Pitaevskii equation, where the nonlinear interaction term is a function of the local density. In the case of a harmonic trapping potential in the radial direction with trapping frequency $\omega_\perp$, the effective 1D equation of motion is

$$i\hbar \frac{d}{dt}\psi(z) = \left[\frac{-\hbar^2}{2m}\frac{\partial^2}{\partial z^2} + V(z) + \frac{U_{3d}}{2\pi\sigma^2}|\psi(z)|^2 \right. $$
$$\left. + \left(\frac{\hbar^2}{2m}\sigma^{-2} + \frac{m\omega_\perp^2}{2}\sigma^2 \right) \right]\psi(z), \quad (1)$$

with

$$\sigma^2(z) = \frac{\hbar}{m\omega_\perp}\sqrt{1 + 2a_s|\psi(z)|^2}. \quad (2)$$

$V(z)$ represents the external potential along the z direction, $U_{3d}=4\pi\hbar^2 a_s/m$ is the $3d$ atom-atom interaction strength, and a_s is the s-wave scattering length. We solve this equation numerically with no free parameters.

A. Case 1

We used Eqs. (1) and (2) to simulate the experimental conditions used in case 1. We used an initial condition of 50 million atoms in the ground state of a harmonic trap of trapping frequencies $\omega_z=2\pi\times3.9$ Hz and $\omega_\perp=2\pi\times97$ Hz. The ground state was found by imaginary time propagation. A repulsive potential due to the laser beam was then switched on. The laser power was 49 mW and detuned by 23 nm from resonance. We assumed that the beam profile was Gaussian with a width of 90 μm. This corresponds to a repulsive potential height of 0.87 μK.

Figure 3 shows a comparison of theoretical calculations with experimental data for these parameters. The left column [(a)–(d)] shows the density profile of the condensate, integrated along the radial direction, and the right column [(e)–(h)] shows the theoretical calculations. The images are for (a) and (e) 11 ms, (b) and (f) 14 ms, (c) and (g) 21 ms, and (d) and (h) 32 ms after the repulsive potential were switched on.

The experimental images show that we get two pulses propagating outward. The leading edges of these pulses get steeper due to the density-dependent speed of sound [27]. The theoretical plots show agreement with the experimental data in terms of the position of the pulses and the steepening of the density. However, they show extra detail, which the experimental image is insufficient to resolve. As the pulses steepen, the relative density gradient becomes comparable to the healing length, and a shock wave forms. This causes an abrupt change in the density profile of the smooth pulse, resulting in rapid density oscillations in front and behind the pulse. Figure 4 compares the relative density gradient
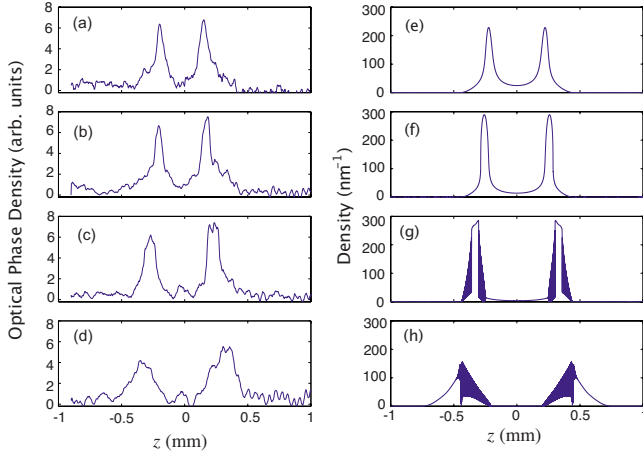
FIG. 3. (Color online) Comparison of theoretical calculations with experimental data. The left column [(a)–(d)] shows the density profile of the condensate, integrated along the radial direction, and the right column [(e)–(h)] shows the theoretical calculations. The images are for (a) and (e) 11 ms, (b) and (f) 14 ms, (c) and (g) 21 ms, and (d) and (h) 32 ms after the repulsive potential was switched on. The laser power was 49 mW, which corresponds to a repulsive potential height of 0.87 μK.

$$g(z) \equiv \frac{\frac{dn(z)}{dz}}{n(z)}, \qquad (3)$$

to the inverse of the healing length

$$k_{wb}(z) \equiv \frac{1}{\xi} = \frac{\sqrt{2mn(z)U(z)}}{\hbar}, \qquad (4)$$

where $U(z) = U_{3d}/2\pi\sigma^2(z)$ is the effective 1D interaction strength. In (a) and (d), $|g(z)| \ll k_{wb}(z)$, and the density profile

of the pulse remains smooth. In (b) and (e), $|g(z)|$ becomes comparable to $k_{wb}(z)$, and a shock front begins to form. In (c) and (f), $|g(z)| \gg k_{wb}$, and high-frequency oscillations are visible in the density profile.

We found similar agreement between theoretical results and experimental data for repulsive barrier heights of 0.39 and 3.27 μK (corresponding to data presented in Fig. 1), which we have not presented here.

B. Case 2

In the second set of data, we made use of time-of-flight imaging and were able to observe features that were not resolvable in trap. To make a comparison with this experimental data, we have modeled the expansion of the condensate in the radial direction during time of flight combined with continuing the 1D simulation of the dynamics of the wave function in the axial direction. We are unable to use the NPGPE in this case, as it is unable to model the expansion in the radial direction. Instead, we obtained a 1D set of equations by assuming a transverse radial width of the condensate, which was independent of z, which allowed us to scale our nonlinearity to one dimension using $U_{1d} = U_{3d}/\pi R^2$. We chose this width parameter R by comparing the evolution, while still in the trap to the evolution of the NPGPE with no free parameters, and chose the transverse width parameter, which gave the best agreement in the results. Figure 5 shows the comparison between the solution to the GPE and the NPGPE after 3 ms of evolution, during the trapped phase of the evolution. For the GPE simulation, we set $R = 12$ μm, which gave the best agreement with the NPGPE.

During the expansion phase, we assumed that the transverse width expanded according to the analytic result derived by Castin and Dum [43] for the self-similar expansion of a Thomas-Fermi condensate. According to this result, the
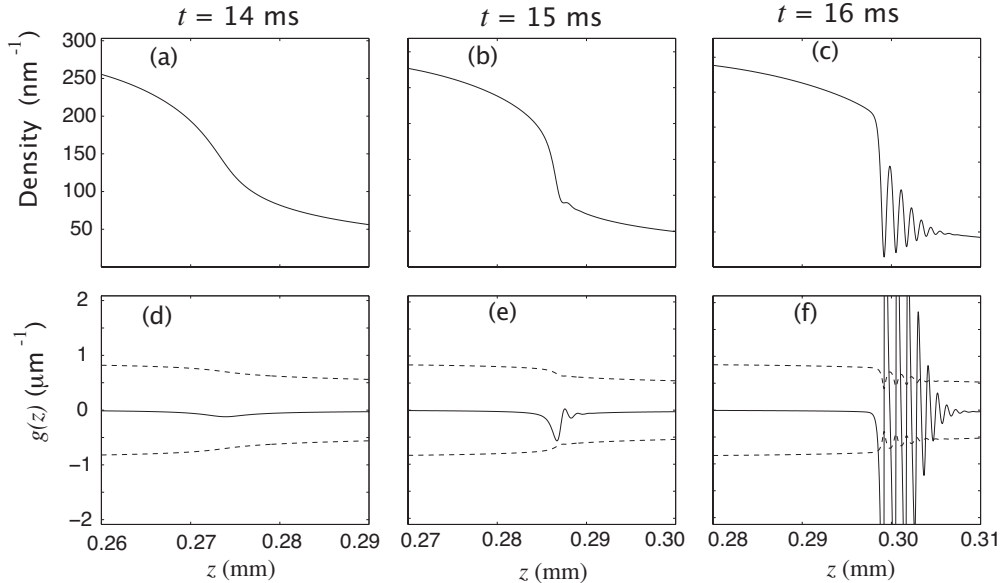

FIG. 4. Top row: closeup of the density profile of the leading edge of the pulse for (a) $t = 14$ ms, (b) $t = 15$ ms, and (c) $t = 16$ ms, for the same parameters as 3. Bottom row: the relative density gradient, $g(z)$ (solid line), and the inverse of the healing length $\pm k_{wb}(z)$ (dashed line) for the cases in (a), (b), and (c), respectively. In (d), $|g(z)| \ll k_{wb}(z)$, so the pulse propagates smoothly. In (e), $g(z)$ becomes comparable to $k_{wb}(z)$, and a shock front begins to form. In (f), $|g(z)| \gg k_{wb}(z)$, and high-frequency oscillations are visible in the density profile.
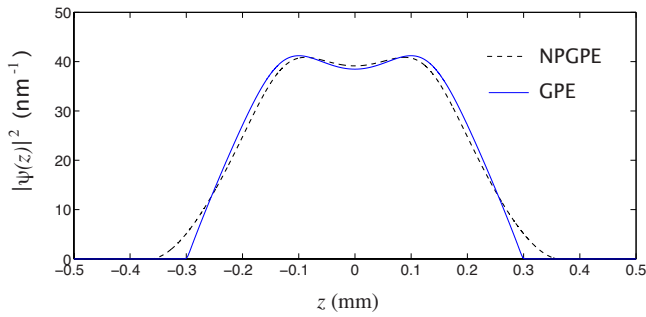
FIG. 5. (Color online) Comparison of the density profiles resulting from GPE (solid line) and NPGPE (dashed line) simulations. The condensate was left to evolve in trap for 3 ms with a 0.88 μK repulsive barrier.

transverse width evolves according to $R(t) = R(0)\sqrt{1 + (\omega_\perp t)^2}$. As we have neglected to include three-dimensional effects in our simulation, we do not expect perfect agreement with the experimental data.

Figure 6 shows the density slice from the experimental data from Fig. 2 (integrated in the y direction for 100 pixels) compared to theoretical simulations. There is excellent agreement between these results. In both cases, high contrast fringes are observed when the back edge of the pulse catches up with the front edge. We find that the wave breaking occurs after a much shorter time compared to the case I because the expansion in the radial direction leads to a rapid increase in the healing length.

There is considerable agreement between our simulation with no free parameters, and the experimental data, indicating that it is valid to simulate such a violent system with the GPE. The main cause of discrepancy between the experimental images and the theoretical calculations is most likely the uncertainty in the size of the waist of the blue-detuned beam $(90 \pm 11 \ \mu$m). By adjusting the value of the waist slightly in the calculations, we found better agreement with the experimental images, with the positions and widths of the wave packets giving best agreement for a waist of 92 μm. There is also a slight discrepancy in the spatial frequency of the interference fringes for the experimental images and the simulation; the cause of which is unknown. It is difficult to accurately determine the spatial frequency in the experimental images, due to the 3 μm pixel size causing spatial aliasing. The drop in observed fringe contrast in the experimental images is partly due to this spatial aliasing effect, but most likely is the result of a slight misalignment of the imaging axis with respect to the axis of the fringes in the three-dimensional experiment. The asymmetry is due to a slight misalignment of the dipole barrier with the center of the trap. Figure 7 shows a comparison between the experimental data, and the results from the simulation convolved with a Gaussian of width 3 μm, to emulate the effect of the 3 μm resolution. The fringe contrast is reduced as a result of the convolution, especially toward the back end of the pulse, where the fringe separation is smaller. However, this effect is not enough to describe the lack of fringe contrast in the experimental images at the front of the pulse. One might suspect
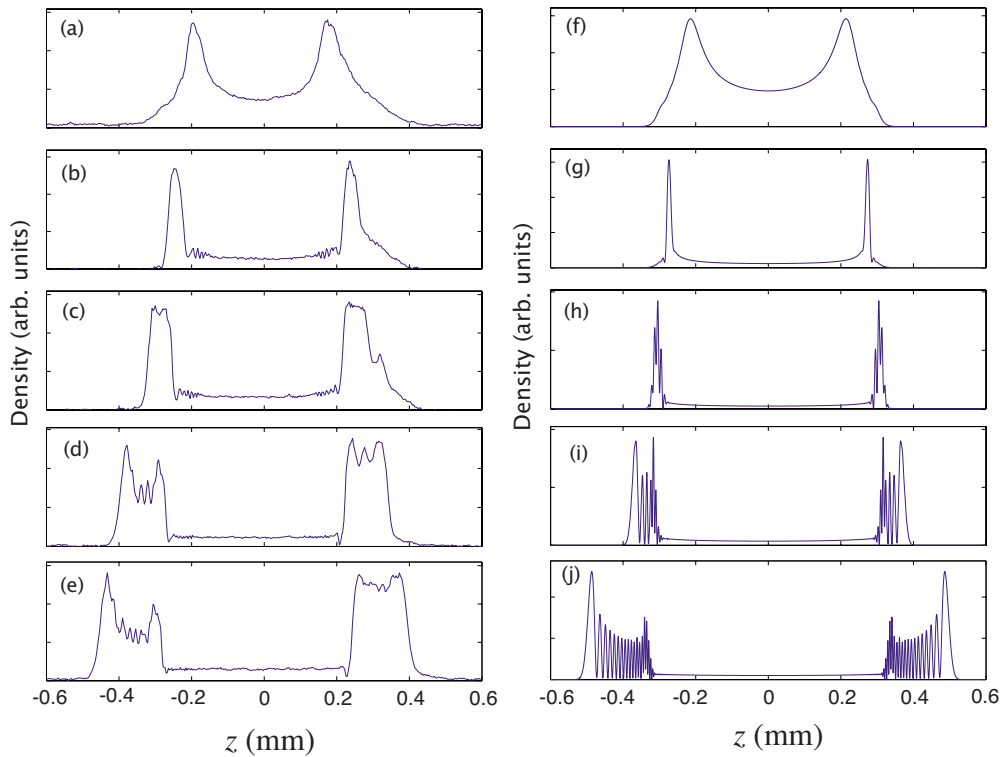

FIG. 6. (Color online) Density slice (left column) and theoretical 1D GPE simulation (right column) of the density profile of the condensate after expansion for 69 ms after evolving in the trap for various times. The condensate was held in the trap with the optical dipole on potential for (a) and (f) 0.5 ms, (b) and (g) 1.1 ms, (c) and (h) 1.5 ms, (d) and (i) 2.0 ms, and (e) and (j) 3.0 ms. Parameters: $N = 1.8 \times 10^7$, waist=90 μm, P=21 mW, and detuning=10 nm, corresponding to a barrier height of 0.88 μK.
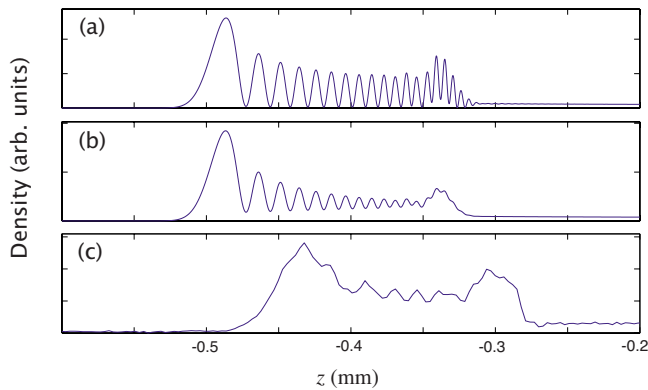
FIG. 7. (Color online) Closeup view of the density slice for the same conditions as Figs. 6(e) and 6(j). (a) shows the raw simulation data, (b) shows the same data convolved with a 3 μm Gaussian to emulate the finite pixel size of the camera, and (c) shows the experimental data. The discrepancy in the positions of the experimental and theoretical density distributions is most likely due to the uncertainty in the waist of the blue-detuned beam.

that the reduced fringe visibility is due to heating of the condensate atoms. However, no thermal fraction was observed. This was validated by repeating the experiment for different expansion times. Inspection of Fig. 2 shows that the wave front of the leading edge of the pulse is slightly curved. As this curvature will also be present in the direction of imaging, this may also contribute to the loss of fringe visibility. However, we cannot confirm that this is the cause of the loss of fringe visibility, as our 1D model does not capture

this curvature. Given these discrepancies, it is clear that the solutions of the GPE correctly capture the physical processes determining the evolution of the system.

IV. CONCLUSION

We have generated shock waves in a large number elongated Bose-Einstein condensate by suddenly splitting it with a blue-detuned optical dipole potential. We observe no significant particle loss or heating over these time scales and find excellent agreement with the predictions of our simulations of the 1D nonpolynomial Gross-Pitaevskii equation. We used a method to describe the expansion of the elongated condensate while simulating the continuing dynamics in the long direction and, again, find excellent agreement with simulations. Our study provides further evidence that the Gross-Pitaevskii equation can be an excellent approximation to the dynamics of condensates even in situations exhibiting violent dynamics and low dissipation.

[1] M. H. Anderson, J. R. Ensher, M. R. Matthews, C. E. Wieman, and E. A. Cornell, Science **269**, 198 (1995).

[2] F. Dalfovo, S. Giorgini, L. P. Pitaevskii, and S. Stringari, Rev. Mod. Phys. **71**, 463 (1999).

[3] M. Edwards, P. A. Ruprecht, K. Burnett, R. J. Dodd, and C. W. Clark, Phys. Rev. Lett. **77**, 1671 (1996).

[4] S. Burger, K. Bongs, S. Dettmer, W. Ertmer, K. Sengstock, A. Sanpera, G. V. Shlyapnikov, and M. Lewenstein, Phys. Rev. Lett. **83**, 5198 (1999).

[5] M. Trippenbach, Y. B. Band, and P. S. Julienne, Phys. Rev. A **62**, 023608 (2000).

[6] Z. Dutton, M. Budde, C. Slowe, and L. V. Hau, Science **293**, 663 (2001).

[7] V. Y. F. Leung, A. G. Truscott, and K. G. H. Baldwin, Phys. Rev. A **66**, 061602(R) (2002).

[8] N. Katz, R. Ozeri, J. Steinhauer, N. Davidson, C. Tozzo, and F. Dalfovo, Phys. Rev. Lett. **93**, 220403 (2004).

[9] N. P. Robins, C. M. Savage, J. J. Hope, J. E. Lye, C. S. Fletcher, S. A. Haine, and J. D. Close, Phys. Rev. A **69**, 051602 (2004).

[10] N. P. Robins, A. K. Morrison, J. J. Hope, and J. D. Close, Phys. Rev. A **72**, 031606 (2005).

[11] M. Kohl, Th. Busch, K. Molmer, T. W. Hansch, and T. Esslinger, Phys. Rev. A **72**, 063618 (2005).

[12] J. E. Lye, L. Fallani, M. Modugno, D. S. Wiersma, C. Fort, and M. Inguscio, Phys. Rev. Lett. **95**, 070401 (2005).

[13] D. Ananikian and T. Bergeman, Phys. Rev. A **73**, 013604 (2006).

[14] C. J. Pethick and H. Smith, *Bose-Einstein Condensation in Dilute Gases* (Cambridge University Press, New York, 2001).

[15] A. A. Norrie, R. J. Ballagh, and C. W. Gardiner, Phys. Rev. A **73**, 043617 (2006).

[16] E. A. Donley, N. R. Claussen, S. L. Cornish, J. L. Roberts, E. A. Cornell, and C. E. Wieman, Nature (London) **412**, 295 (2001).

[17] H. Saito and M. Ueda, Phys. Rev. A **65**, 033624 (2002).

[18] S. K. Adhikari, Phys. Lett. A **296**, 145 (2002).

[19] L. Santos and G. V. Shlyapnikov, Phys. Rev. A **66**, 011602(R) (2002).

[20] C. M. Savage, N. P. Robins, and J. J. Hope, Phys. Rev. A **67**, 014304 (2003).

[21] S. Wüster, J. J. Hope, and C. M. Savage, Phys. Rev. A **71**, 033604 (2005).

[22] S. Wüster, B. J. Dąbrowska-Wüster, A. S. Bradley, M. J. Davis, P. B. Blakie, J. J. Hope, and C. M. Savage, Phys. Rev. A **75**, 043611 (2007).

[23] S. L. Cornish, S. T. Thompson, and C. E. Wieman, Phys. Rev. Lett. **96**, 170401 (2006).

[24] B. Dabrowska-Wüster, S. Wüster, and M. Davis, New J. Phys. **11**, 053017 (2009).

[25] K. E. Strecker, G. B. Partridge, A. G. Truscott, and R. G. Hulet, Nature (London) **417**, 150 (2002).

[26] L. Khaykovich, F. Schreck, G. Ferrari, T. Bourdel, J. Cubizolles, L. D. Carr, Y. Castin, and C. Salomon, Science **296**, 1290 (2002).

[27] B. Damski, Phys. Rev. A **69**, 043610 (2004).

[28] K. E. Strecker, G. B. Partridge, A. G. Truscott, and R. G. Hulet, New J. Phys. **5**, 73 (2003).

[29] U. Al Khawaja, H. T. C. Stoof, R. G. Hulet, K. E. Strecker, and G. B. Partridge, Phys. Rev. Lett. **89**, 200404 (2002).

[30] V. M. Perez-Garcia, V. V. Konotop, and V. A. Brazhnyi, Phys. Rev. Lett. **92**, 220403 (2004).

[31] T. Frisch, Y. Pomeau, and S. Rica, Phys. Rev. Lett. **69**, 1644 (1992).

[32] T. Winiecki, J. F. McCann, and C. S. Adams, Phys. Rev. Lett. **82**, 5186 (1999).

[33] R. Carretero-González, P. G. Kevrekidis, D. J. Frantzeskakis, B. A. Malomed, S. Nandi, and A. R. Bishop, Math. Comput. Simul. **74**, 361 (2007).

[34] R. G. Scott and D. A. W. Hutchinson, Phys. Rev. A, **78**, 063614 (2008).

[35] T. P. Simula, P. Engels, I. Coddington, V. Schweikhard, E. A. Cornell, and R. J. Ballagh, Phys. Rev. Lett. **94**, 080404 (2005).

[36] M. A. Hoefer, M. J. Ablowitz, I. Coddington, E. A. Cornell, P. Engels, and V. Schweikhard, Phys. Rev. A **74**, 023623 (2006).

[37] M. A. Hoefer, M. J. Ablowitz, and P. Engels, Phys. Rev. Lett. **100**, 084504 (2008).

[38] J. J. Chang, P. Engels, and M. A. Hoefer, Phys. Rev. Lett. **101**, 170404 (2008).

[39] S. A. Morgan, R. J. Ballagh, and K. Burnett, Phys. Rev. A **55**, 4338 (1997).

[40] K. M. R. van der Stam, E. D. van Ooijen, R. Meppelink, J. M. Vogels, and P. van der Straten, Rev. Sci. Instrum. **78**, 013102 (2007).

[41] M. R. Andrews, M.-O. Mewes, N. J. van Druten, D. S. Durfee, D. M. Kurn, and W. Ketterle, Science **273**, 84 (1996).

[42] L. Salasnich, A. Parola, and L. Reatto, Phys. Rev. A **65**, 043614 (2002).

[43] Y. Castin and R. Dum, Phys. Rev. Lett. **77**, 5315 (1996).